PERGAMON

Carbon 38 (2000) 1741–1744

CARBON

STM study of single-walled carbon nanotubes

Philip Kim*, Teri W. Odom, Jinlin Huang, Charles M. Lieber

Harvard University, Cambridge, MA 02138, USA

Abstract

The electronic density of states of atomically resolved single-walled carbon nanotubes (SWNTs) have been investigated using scanning tunneling microscopy (STM). Peaks in the density of states due to the one-dimensional nanotube band structure have been characterized and compared with the results of tight-binding calculations. © 2000 Published by Elsevier Science Ltd.

Keywords: A. Carbon nanotubes; C. Scanning tunneling microscopy (STM)

1. Introduction

STM has proved to be a particularly suitable probe for carbon nanotubes, since it can resolve simultaneously both the atomic structure and the electronic DOS. The recent development of techniques to produce and purify relatively large quantities of SWNTs [1,2] has made it possible to perform high resolution STM experiments probing electronic properties of SWNTs. Indeed, low temperature STM experiments [3,4] have resolved the atomic structure and electronic density of states of purified SWNTs, and have confirmed the predicted electronic behavior of SWNTs showing that the electronic properties of SWNTs depend sensitively on diameter and helicity [5–7], and thus the major features of theory were verified. The tunneling spectra reported in these low temperature STM studies exhibited peaks in the density of states (DOS), van Hove singularities (VHS), which are believed to reflect the 1D band structure of SWNTs. A detailed experimental comparison with theory was carried out in recent experimental work [8] correlating atomic structure of SWNTs with the electronic local density of states (LDOS) quantitatively.

2. STM experiments and analysis

SWNTs were grown by pulsed laser vaporization methods. Samples suitable for STM and STS studies were prepared by spin coating a suspension of the purified SWNTs in dichloroethane onto a Au(111) surface. Immediately after SWNT deposition onto freshly prepared Au(111)/mica substrate, the sample was loaded into a UHV STM that was stabilized at 77 K or 4 K.

The structural (n, m) indices of a SWNT [9] are obtained from the experimentally determined values of the chiral angle, θ_{exp}, and the diameter, D_{exp}. For a SWNT, the chiral angle θ and the diameter D can be related to the (n, m) of the tube. However, the relations of θ vs. θ_{exp} and D vs. D_{exp} are rather subtle due to the fact that STM images are a convolution of the tip shape and samples. Therefore, careful considerations are required to extract θ and D from θ_{exp} and D_{exp}.

The experimental chiral angle θ_{exp} was measured between the (n, n) direction and the central tube axis for $\theta_{exp} < 15°$. Because the tube axis is perpendicular to $\mathbf{C_h}$, this angle is equivalent to the angle between (n, 0) and $\mathbf{C_h}$, as θ was originally defined. When $\theta_{exp} > 15°$, the angle ϕ between the (n, 0) and the tube axis was measured, and θ_{exp} was determined from $\theta_{exp} = 30° - \phi$. This approach confines our angle measurements to the best defined atomic structure at the top of the SWNTs, and thus minimizes contributions from the structure at the sides of the highly curved tubes, since the latter can be distorted by the finite size and asymmetry of the tip. In a recent theoretical study, Meunier et al. [10] pointed out that care should be taken to relate θ_{exp}, measured from a STM image, to the real chiral angle θ of the SWNT. SWNT STM images were simulated in their study using a tight-binding calculation treating the STM

*Corresponding author.
E-mail address: pkim@socrates.berkeley.edu (P. Kim).

0008-6223/00/$ – see front matter
PII: S0008-6223(99)00298-5

tip as a point-like object. θ and θ_{exp} in the simulation were related by

$$\theta_{exp} \approx \left(1 + \frac{h}{R}\right)\theta, \quad (1)$$

where h is the tip–SWNT separation and R is the radius of the SWNT. This simple relation is based on an inflation of simulated STM images perpendicular to the tube axis due to the fact that the point-like tip follows the constant LDOS surface which is a distance $R + h$ away from the tube center (Fig. 1a). However, in real STM experiments, the situation is more complicated than the simulation, because of the finite dimensions of the STM tip. With the condition

$$r_t \sim h \ll R, \quad (2)$$

where r_t is the effective radius of the STM tip, the distortion of the STM image may be quite small at the top of the curved surface, and thus, $\theta_{exp} \approx \theta$. We speculate that Eq. (1) fails to hold, because within such a proximity condition ($r_t \sim h$), the perturbative approach with a point-like tip [10] may not work. Indeed, most of our high resolution SWNT STM images, which presumably satisfy Eq. (2), do not show any appreciable distortions. Fig. 1b shows examples of high resolution SWNT STM images. Model SWNT structures, whose (n, m) indices were determined using $\theta \approx \theta_{exp}$ and the diameter derived from cross-section analysis (described below), were generated, and then 2D projections of these 3D SWNT models were directly overlaid on the STM images for comparison. As shown in the figure, SWNT images match well with a projection of the model SWNT (black hexagons) exhibiting no appreciable distortion, especially at the top surface. It was also found that the apparent height of SWNT from the cross-section of STM scan line is 2–6 Å (see, for example, Fig. 1d). From this value we estimate $h \lesssim 2$ Å, which satisfies Eq. (2).

However, we found that lower resolution images do exhibit distortion of hexagonal atomic arrays in the STM image perpendicular to the tube axis. We believe that this distortion is due to the effects of a relatively blunt tip. Fig. 1c shows an example of this lower resolution SWNT image. Hexagons laid over the top panel (raw STM image) show an apparent stretching in the y-axis (the direction perpendicular to the tube axis). To correct for this tip-induced effect, we rescale the image along the y-axis, and obtain regular hexagons overlaid at the top of the tube surface (lower panel). From the rescale factor, the ratio, h/R, which appears in Eq. (1), is estimated to be ~ 0.2 for

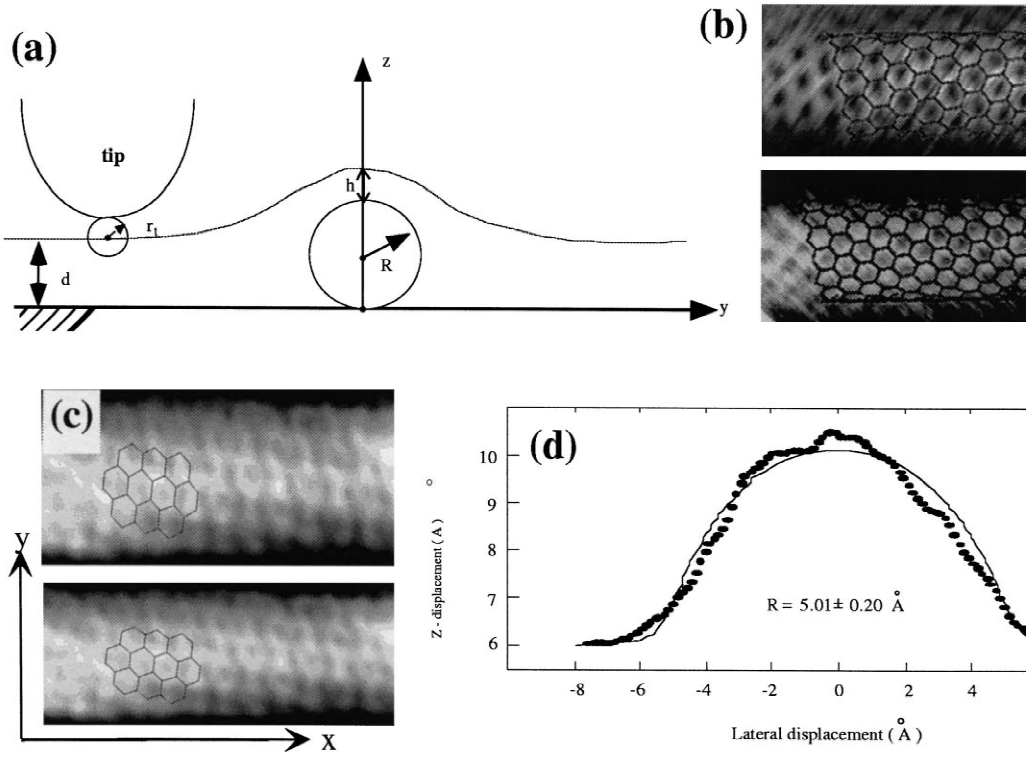

Fig. 1. (a) A model situation of STM tip and SWNT. (b) A high resolution SWNT STM image and projection of ideal tube. (c) A low resolution distorted STM image and correction of the inflation effect. (d) Average cross section of scan line of SWNT STM image and fitting to Eq. (3).

this image. In our procedure to obtain θ from θ_{exp} in a lower resolution image (or distorted image), the image was rescaled to deconvolute tip-induced effects in θ_{exp} (Eq. (1)).

SWNT diameters were determined from the cross-sections of nanotube images after deconvoluting the tip contribution to the image. An overall cross-section was assigned by averaging ~400 scan lines for each nanotube (Fig. 1d). This representative cross-section exhibits a smooth half circle curve, and thus in the first approximation, we considered the SWNT to be a cylinder of radius R, which will be determined from the curve. Fig. 1a represents the tunneling model used in the deconvolution calculation which assumes a spherical shape STM tip. A phenomenological form of the tunneling current for this model can be written as

$$\begin{cases} I = I_g \exp(-k_g z) + I_t \exp\left(-k_t\sqrt{y^2 + (z-R)^2}\right) & \text{near SWNT} \\ I = I_g \exp(-k_g d) & \text{as } y \to \infty, \end{cases} \quad (3)$$

where k_g, k_t, and d are the inverse decay length on gold, the inverse decay length on the tube, and the tip to gold distance when the tip is far away from the SWNT, respectively. I_t and I_g contain the complicated geometric and electronic structure of both the tip and the tube, which serve as fitting parameters. This equation is then used to fit the average cross-section mentioned above to obtain the SWNT diameter $2R$ (Fig. 1d). The parameters obtained from this model are reasonable and are in agreement with those obtained from Au steps in the same experiments. The typical uncertainty in SWNT diameter from high-resolution STM images is ± 0.05 nm. We believe that this approach yields a more robust diameter measurement than the diameter determination from the apparent height or width only, since the apparent height is highly-dependent on imaging conditions such as bias voltage while the apparent width contains primarily tip convolution effects.

3. Results and discussion

An atomically resolved STM image of several SWNTs is shown in Fig. 2a. The diameter and chiral angle measured following the method described in the previous section for this tube are 1.35 ± 0.1 nm and $-20 \pm 1°$, respectively. We find that the (13, 7) indices are the best description of the tube.

Indeed, the STS data shows relatively good agreement with the DOS for a (13, 7) tube calculated using the zone-folding approach (Fig. 2b). The agreement between the VHS positions determined from our dI/dV data and calculations are especially good below the Fermi energy (E_F) where the first seven peaks correspond well. Above E_F, larger deviations between experimental data and calculations exist. The observed differences may be due to band repulsion, which arises from the curvature-induced hybridization, or surface-tube interaction that were not accounted for in our calculations. Detailed ab initio [11] calculations have shown that the effect of curvature induced by hybridization is much higher in π^*/σ^* than π/σ orbitals. Bands above E_F are thus more susceptible to the hybridization effect, and this could explain the greater deviations between experiments and calculation that we observe for the empty states.

In addition, we have investigated the sensitivity of the DOS to (n, m) indices. Specifically, we calculated the DOS of the next closest metallic SWNT to our experimental diameter and angle; that is a (12, 6) tube. Significantly, we find that the calculated VHS for this (12, 6) tube deviates much more from the experimental DOS peaks than in the

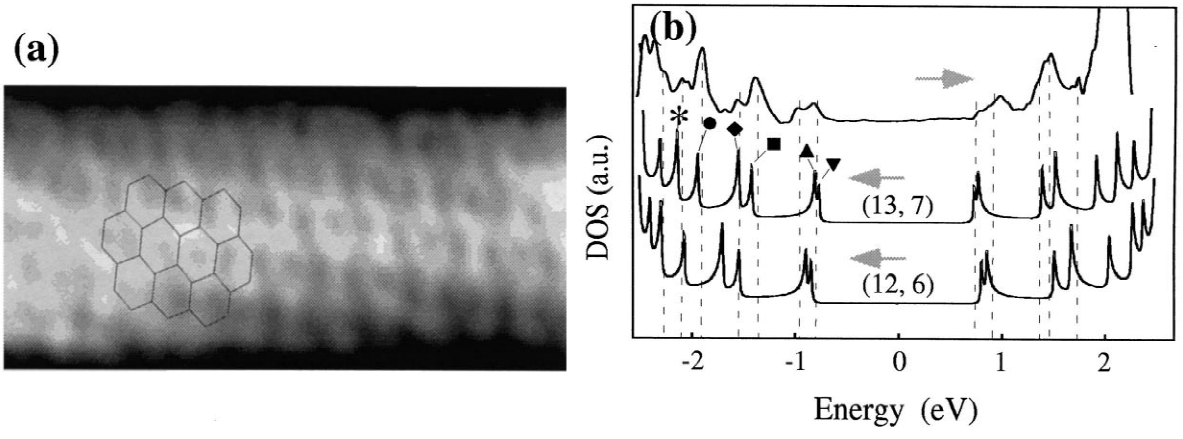

Fig. 2. (a) STM image of SWNTs recorded at $I = 0.12$ nA and $V = 550$ mV. A portion of a hexagonal lattice is overlaid to guide the eye. (b) Comparison of DOS obtained from our experiment (upper curve) and π-only tight binding calculation for (13, 7) SWNT (the second curve from top). The broken vertical lines indicate the positions of VHS in the tunneling spectra. The symbols correspond to the VHS shown in (a). The calculated DOS of (12, 6) are included for comparison.

case of the (13, 7) tube (Fig. 2b). We believe that this analysis not only substantiates our assignment of the indices in Fig. 2a, but more importantly, demonstrates the sensitivity of the DOS to subtle variations in diameter and chirality.

4. Summary

We have presented STM and STS characterizations of the atomic structure and electronic DOS of SWNTs. We have observed sharp VHS in the LDOS of atomically-resolved SWNTs at larger energy scales, which were compared to tight-binding calculations for specific tube indices. Remarkably good agreement was obtained between experiment and π-only calculations, although deviations suggest that further work will be required to understand fully the band structure of SWNTs in contact with surfaces.

References

[1] Thess A et al. Science 1996;283:483.
[2] Journet C et al. Nature 1997;388:756.
[3] Wilder JWG et al. Nature 1998;391:59.
[4] Odom TW et al. Nature 1998;391:61.
[5] Mintmire JW et al. Phys Rev Lett 1992;68:631.
[6] Hamada N et al. Phys Rev Lett 1992;68:1579.
[7] Saito R et al. Appl Phys Lett 1992;60:2204.
[8] Kim P et al. Phys Rev Lett 1999;82:1225.
[9] Dresselhaus MS et al. Science of fullerenes and carbon nanotubes, San Diego: Academic, 1996.
[10] Meunier V et al. Phys Rev Lett 1998;81:5588.
[11] Blase X et al. Phys Rev Lett 1994;72:1878.